Synthesis, Reactivities, and Electrochemical Properties of Pyridinecarboxamide Complexes of Rhodium(III) and Iridium(III). Crystal Structure of $[Rh(bpb)(py)_2]ClO_4$ [H_2bpb = 1,2-bis(2-pyridinecarboxamido)benzene, py = pyridine]†

Shing-Tat Mak, Vivian Wing-Wah Yam, and Chi-Ming Che*
Department of Chemistry, University of Hong Kong, Pokfulam Road, Hong Kong
Thomas C. W. Mak
Department of Chemistry, the Chinese University of Hong Kong, Shatin, New Territories, Hong Kong

A series of organo and non-organo rhodium and iridium complexes of bpb and bpc ligands [H_2bpb = 1,2-bis(2-pyridinecarboxamido)benzene, H_2bpc = 4,5-dichloro-1,2-bis(2-pyridinecarboxamido)benzene] have been synthesized. These complexes display reversible one-electron oxidation couples. Stable one-electron-oxidized species have been generated both chemically and electrochemically. The oxidation potentials are affected dominantly by the charge effect but are relatively independent of the nature of the central metal ions and axial ligands. On the contrary, $[Rh(bpe)R]\cdot H_2O$ complexes [R = Me or Et; H_2bpe = 1,2-bis(2-pyridinecarboxamido)ethane] can only be oxidized irreversibly at a potential of about 0.3 V more anodic than that of the corresponding bpb complexes. The involvement of the equatorial ligand in the oxidation of the bpb and bpc complexes has been suggested. The complex $[Rh(bpb)(py)_2]ClO_4$ has been characterized by *X*-ray crystallography: space group $P\bar{1}$, a = 8.316(1), b = 9.620(2), c = 17.405(6) Å, α = 98.87(2), β = 99.57(2), γ = 90.55(2)°, Z = 2, and R = 0.039 for 4 788 observed reflections.

Recent studies on the oxidation chemistry of high-valent iridium complexes[1] have drawn our attention toward the high-valent chemistry of the analogous cobalt and rhodium complexes. The studies by Halpern and co-workers[2] suggested that organocobalt(IV) and organorhodium(IV) could be stabilized by dianionic chelating ligands. We found that dianionic pyridine-containing amide ligands are also capable of stabilizing transition-metal ions in high oxidation states. The close resemblance of amide groups to peptide linkages in proteins also aroused our interest in their co-ordination chemistry. In this contribution we report the synthesis and characterization of a series of complexes of Rh^{III} and Ir^{III} containing pyridine-carboxamide type ligands; their chemical and electrochemical oxidations will also be discussed.

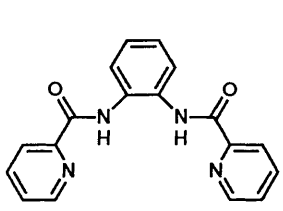

H_2bpb

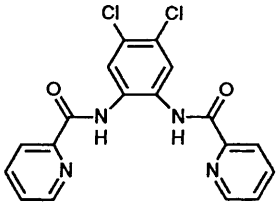

H_2bpc

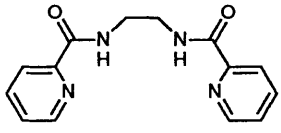

H_2bpe

Experimental

Reagents and Materials.—Rhodium(III) trichloride hydrate was obtained from Aldrich Chemicals Ltd. 1,2-Phenylenediamine was recrystallized from hot ethanol before use. Aluminium oxide (Activity II, BDH Chemicals Ltd.) was used for column chromatography. All other solvents and chemicals used in syntheses were of reagent grade, without further purification.

In electrochemical work, doubly distilled water was used. Acetonitrile (Mallinckrodt, ChromAR) and dichloromethane (Ajax, AR) were distilled from CaH_2 before use. Methanol (Merck, extra pure) was dried by distillation over magnesium. Tetra-n-butylammonium perchlorate, tetrafluoroborate, tetraethylammonium perchlorate, and tetrafluoroborate (Southwestern Analytical Chemicals, Electrometric grade) were dried at 100 °C (60 °C for perchlorates) under vacuum for 24 h before use.

All solutions for electrochemical studies were deaerated with pre-purified argon gas. For electrochemical studies in non-aqueous media (acetonitrile, dichloromethane, and methanol) the argon was dried by passing through sodium hydroxide, then activated molecular sieve (5 Å), and finally presaturated with the solvent used in the electrochemical studies before passage into the electrochemical cell.

Ligand Syntheses.—1,2-Bis(2-pyridinecarboxamido)benzene (H_2bpb) was synthesized by condensation of 1,2-phenylenediamine and pyridine-2-carboxylic acid in pyridine in the presence of triphenyl phosphite.[3] Similarly, 4,5-Dichloro-1,2-bis(2-pyridinecarboxamido)benzene (H_2bpc) was synthesized from 4,5-dichloro-1,2-phenylenediamine and pyridine-2-carboxylic acid, and 1,2-bis(2-pyridinecarboxamido)ethane (H_2bpe) from ethylenediamine and pyridine-2-carboxylic acid. The characterization of the H_2bpb and H_2bpe ligands has been

† *Supplementary data available:* see Instructions for Authors, *J. Chem. Soc., Dalton Trans.*, 1990, Issue 1, pp. xix—xxii.

reported previously.[4] The structure of H_2bpc has been established by *X*-ray crystallography.[5]

Syntheses of Metal Complexes.—Na[Rh(bpb)Cl_2]. The compounds $RhCl_3 \cdot xH_2O$ (0.45 g) and H_2bpb (0.60 g) were refluxed in dimethylformamide (15 cm^3) for 6 h, after which the solvent was distilled off. The residue was washed with diethyl ether, and then dissolved in methanol (50 cm^3) containing NaOH (0.1 g). The solution was filtered and reduced in volume under vacuum to give red microcrystals of Na[Rh(bpb)Cl_2]. The crystals were filtered off and washed with a minimum amount of cold methanol. The crude product was recrystallized from acetonitrile–diethyl ether to give orange flakes. Yield 70% {Found: C, 38.75; H, 2.95; Cl, 12.75; N, 10.05. Calc. for Na[Rh(bpb)Cl_2]·2.5H_2O: C, 38.75; H, 3.05; Cl, 12.70; N, 10.05%}. I.r.: ν(C=O) 1 615 cm^{-1}.

[Rh(bpb)$(py)_2$]ClO_4 *and* [Rh(bpb)(py)Cl]. The compound $RhCl_3 \cdot xH_2O$ (0.2 g) was added to a refluxing methanolic solution (30 cm^3) of H_2bpb. After 2 h the resulting yellow precipitate was collected by filtration and washed with methanol. The yellow solid was then suspended in ethanol at 60 °C. Pyridine (py) (1 cm^3) and zinc powder (0.1 g) were added under an atmosphere of nitrogen. The mixture was stirred for 10 min after which it was filtered and evaporated to dryness under vacuum. The residue was then column chromatographed on alumina (activity II). The complex [Rh(bpb)(py)Cl] was first eluted by chloroform–acetone (1:1 v/v), evaporated to dryness, and recrystallized from hot acetone. Yield 20%. The ion [Rh(bpb)$(py)_2$]$^+$ was eluted with chloroform–methanol (1:1 v/v). Excess of lithium perchlorate was added to the collected fraction and the solution reduced in volume under vacuum to give yellow crystals of [Rh(bpb)$(py)_2$]ClO_4. Orange crystals of [Rh(bpb)$(py)_2$]ClO_4 were obtained by recrystallization from acetonitrile–diethyl ether. Yield 25%. Alternatively, [Rh$(CO)_2Cl_2$] (1 mmol) and H_2bpb (2 mmol) were stirred in methanol containing sodium acetate (0.1 g) under a nitrogen atmosphere. After stirring for 0.5 h, pyridine was added. The solvent was evaporated under reduced pressure. The product [Rh(bpb)(py)Cl] was purified by column chromatography on alumina (activity II) using chloroform–acetone (1:1 v/v) as the eluant and recrystallized from hot acetone {Found: C, 52.05; H, 3.25; N, 12.90. Calc. for [Rh(bpb)$(py)_2$]ClO_4: C, 49.70; H, 3.30; N, 12.40. Found: C, 51.05; H, 3.35; Cl, 7.5; N, 13.30. Calc. for [Rh(bpb)(py)Cl]: C, 51.75; H, 3.20; Cl, 6.65; N, 13.10%}. I.r. [ν(C=O)]; [Rh(bpb)$(py)_2$]ClO_4, 1 635; and [Rh(bpb)(py)Cl], 1 615 cm^{-1}.

[Rh(bpb)$(PPh_3)Cl$] *and* [Rh(bpb)$(PPh_3)_2$]ClO_4. Na[Rh(bpb)Cl_2] (1 mmol) and excess of PPh_3 (5 mmol) were refluxed in ethanol for 2 d. A red precipitate, [Rh(bpb)$(PPh_3)Cl$], was collected by filtration and recrystallized from acetonitrile by diethyl ether diffusion. Lithium perchlorate was added to the filtrate. After slow evaporation of the solvent under reduced pressure, diethyl ether was added to precipitate the red solid [Rh(bpb)$(PPh_3)_2$]ClO_4. Recrystallization using acetonitrile–diethyl ether gave dark red crystals. Alternatively, Na[Rh(bpb)Cl_2] (1 mmol) and excess of PPh_3 (5 mmol) were refluxed in ethanol in the presence of NaOH (0.05 g) for 2 d. After filtration, lithium perchlorate was added to the deep red filtrate. The solvent was reduced in volume under reduced pressure, and diethyl ether was added to precipitate the red solid [Rh(bpb)$(PPh_3)_2$]ClO_4 {Found: C, 61.15; H, 3.90; N, 5.45. Calc. for [Rh(bpb)$(PPh_3)_2$]ClO_4: C, 62.15; H, 4.05; N, 5.35. Found: C, 60.10; H, 3.70; Cl, 4.95; N, 7.85. Calc. for [Rh(bpb)$(PPh_3)Cl$]: C, 60.30; H, 3.80; Cl, 4.95; N, 7.80%}. I.r. [ν(C=O)]: [Rh(bpb)$(PPh_3)_2$]ClO_4, 1 635; and [Rh(bpb)$(PPh_3)Cl$], 1 625 cm^{-1}.

Na[Rh(bpb)$(CN)_2$]. The salt Na[Rh(bpb)Cl_2] (0.2 g) and excess of NaCN (0.1 g) were refluxed in methanol (50 cm^3) for 4 h during which the orange solution turned yellow. After filtering, the filtrate was reduced in volume under vacuum until a yellow solid appeared. The solid was collected by filtration, washed with the minimum amount of cold methanol, and recrystallized from acetone–methanol (1:1 v/v) by diethyl ether diffusion. Yield 75% {Found: C, 46.20; H, 3.05; N, 16.10. Calc. for Na[Rh(bpb)$(CN)_2$]·1.5H_2O: C, 46.10; H, 2.90; N, 16.10%}. I.r.: ν(C=O) 1 620 cm^{-1}.

[Rh(bpb)R]·H_2O (R = Me, Et, *or* Pr^i). The salt Na[Rh(bpb)Cl_2] (0.2 g) was dissolved in a methanolic solution of sodium hydroxide (0.1 g in 40 cm^3). After deoxygenation with nitrogen gas, excess of $NaBH_4$ (0.1 g) was added. The orange solution gradually turned brown and after 0.5 h a brown suspension was obtained. The appropriate alkyl iodide (0.5 cm^3) was added, and the suspended solid redissolved to form a reddish solution. Excess of $NaBH_4$ was destroyed by addition of concentrated HCl. The solution was evaporated to dryness under reduced pressure to give the crude product, which was column chromatographed on alumina (activity II) using chloroform–acetonitrile (1:1 v/v) as the eluant. The collected fractions were evaporated to dryness and the residue was recrystallized from acetonitrile–diethyl ether. Yield 60% {Found: C, 52.30; H, 4.20; N, 12.20. Calc. for [Rh(bpb)Me]·MeOH: C, 51.50; H, 4.10; N, 12.00. Found: C, 53.30; H, 4.05; N, 12.70. Calc. for [Rh(bpb)Et]: C, 53.60; H, 3.80; N, 12.50. Found: C, 52.40; H, 4.40; N, 12.05. Calc. for [Rh(bpb)Pr^i]·H_2O: C, 52.50; H, 4.40; N, 11.65%}. I.r. [ν(C=O)]: [Rh(bpb)Me]·MeOH, 1 610; [Rh(bpb)-Et], 1 610; and [Rh(bpb)Pr^i]·H_2O, 1 610 cm^{-1}.

[Rh(bpb){CH(Me)(Ph)}]·H_2O. The salt Na[Rh(bpb)Cl_2] (0.2 g) was dissolved in a methanolic solution of sodium hydroxide (0.1 g in 40 cm^3). After deoxygenation with nitrogen gas, excess of $NaBH_4$ (0.1 g) was added. After 0.5 h the resulting brown suspension was heated to 50 °C. Styrene (0.5 cm^3) was added and stirred for an additional 2 h. The resulting orange solution was evaporated to dryness, and the residue was column chromatographed on alumina with acetone as the eluant. The product was recrystallized from acetone. Yield 45% (Found: C, 56.60; H, 4.15; N, 10.45. Calc. for [Rh(bpb){CH(Me)(Ph)}]·H_2O: C, 57.60; H, 4.25; N, 10.35%).

Na[Rh(bpc)Cl_2]. The compounds $RhCl_3 \cdot xH_2O$ (0.2 g), H_2bpc (0.3 g), and NaCl (0.05 g) were refluxed in dimethylformamide for 5 h. The solvent was distilled off and the residue washed with diethyl ether. The residue was then dissolved in warm methanol and filtered. The red filtrate was reduced in volume under reduced pressure until a red precipitate appeared. The solid was filtered off, washed with the minimum amount of cold methanol, and recrystallized from acetonitrile–diethyl ether to give red crystals. Yield 75% {Found: C, 35.70; H, 2.95; Cl, 23.50; N, 9.45. Calc. for Na[Rh(bpc)Cl_2]·1.5H_2O: C, 35.45; H, 2.15; Cl, 23.30; N, 9.20%}. I.r.: ν(C=O) 1 620 cm^{-1}.

Na[Rh(bpc)$(CN)_2$]. The salt Na[Rh(bpc)Cl_2] (1 mmol) and NaCN (3 mmol) were refluxed in methanol (50 cm^3) for 4 h during which the orange solution turned yellow. The solution was filtered and the filtrate reduced in volume under vacuum until a yellow precipitate appeared. The precipitate was collected by filtration, washed with the minimum amount of cold methanol, and recrystallized from methanol–acetonitrile (1:1 v/v) by diethyl ether diffusion. Yield 85% {Found: C, 39.90; H, 2.35; Cl, 12.10; N, 14.15. Calc. for Na[Rh(bpc)$(CN)_2$]·2H_2O: C, 40.10; H, 2.35; Cl, 11.85; N, 14.05%}. I.r.: ν(C=O) 1 610 cm^{-1}.

[Rh(bpc)R]·H_2O (R = Me *or* Et). The salt Na[Rh(bpc)Cl_2] (0.2 g) was dissolved in a methanolic solution of NaOH (0.05 g in 50 cm^3) at 50 °C. Excess of $NaBH_4$ (0.1 g) was added under an atmosphere of nitrogen. The reaction mixture was stirred for 45 min, and the resulting black suspension cooled to room temperature. Alkyl iodide (1 cm^3) was added and the suspension gradually redissolved to give a red solution. Concentrated HCl was added to destroy the excess of $NaBH_4$. The solution was

filtered and evaporated to dryness under vacuum. The product was purified by column chromatography on alumina with acetone–chloroform (1:1 v/v) as the eluant. The collected fraction was evaporated to dryness and the solid recrystallized from acetone. Yield 75% {Found: C, 44.20; H, 3.05; Cl, 13.65; N, 11.15. Calc. for [Rh(bpc)Me]·H_2O: C, 43.80; H, 2.90; Cl, 13.60; N, 10.75. Found: C, 44.40; H, 3.30; Cl, 13.80; N, 10.55. Calc. for [Rh(bpc)Et]·H_2O: C, 44.90; H, 3.20; Cl, 13.25; N, 10.45%}. I.r. [ν(C=O)]: [Rh(bpc)Me]·H_2O, 1 615; and [Rh(bpc)Et]·H_2O, 1 615 cm^{-1}.

[Rh(bpe)R]·H_2O (R = Me *or* Et). The compound $RhCl_3$·xH_2O was added to a refluxing solution of H_2bpe in dimethylformamide (dmf). After 10 min the yellow precipitate was collected by filtration, washed with warm dmf and diethyl ether. The yellow solid (0.2 g) was then dissolved in a methanolic solution of NaOH (0.05 g in 20 cm^3). After deoxygenation with nitrogen gas and cooling at 0 °C, excess of $NaBH_4$ (0.1 g) was added. The orange solution gradually turned dark brown. After 15 min the correspondong alkyl iodide (0.5 cm^3) was added, and the solution was stirred for an additional 0.5 h. The orange solution was then filtered and evaporated to dryness under vacuum. The crude product was purified by column chromatography on alumina with acetonitrile–methanol (1:1 v/v) as the eluant. The collected fraction was evaporated to dryness under reduced pressure. Yield 0.1 g. The structure of [Rh(bpe)R]·H_2O was established by ^1H n.m.r. spectroscopy.

Na[Ir(bpb)Cl_2]. The salt $Na_2[IrCl_6]$ (2 mmol) and H_2bpb (2 mmol) were refluxed in dimethylformamide (15 cm^3) for 16 h. The solvent was distilled off and the residue washed with diethyl ether. The product was recrystallized from acetonitrile–diethyl ether to give orange flakes. Yield 70%. {Found: C, 33.10; H, 2.75; Cl, 11.10; N, 8.75. Calc. for Na[Ir(bpb)Cl_2]·3H_2O: C, 32.95; H, 2.75; Cl, 10.80; N, 8.55%}. I.r.: ν(C=O) 1 615 cm^{-1}.

Na[Ir(bpc)Cl_2]. The salt $Na_2[IrCl_6]$ (0.12 g) and H_2bpc (0.1 g) were refluxed in dimethylformamide (15 cm^3) for 16 h. The solvent was distilled off and the residue washed with diethyl ether. The product was recrystallized from acetone to give red crystals. Yield 75% {Found: C, 29.70; H, 2.00; Cl, 20.20; N, 7.25. Calc. for Na[Ir(bpc)Cl_2]·3H_2O: C, 29.80; H, 2.20; Cl, 19.55; N, 7.70%}. I.r.: ν(C=O) 1 620 cm^{-1}.

Physical Measurements and Instrumentation.—Infrared spectra were obtained as Nujol mulls on a Perkin-Elmer 577 spectrophotometer, u.v.–visible spectra on a Shimadzu UV-240 spectrophotometer, and n.m.r. spectra on a JEOL model FX90Q spectrometer (90 MHz). Chemical shifts (δ) are reported relative to tetramethylsilane as internal standard. Elemental analyses of the new complexes were performed either by the Microanalytical unit of the Australian Mineral Development Laboratories or Butterworth Laboratories Ltd.

Cyclic voltammetric measurements were carried out using a Princeton Applied Research (PAR) model 175 universal programmer, model 173 potentiostat, and model 179 digital coulometer coupled to a Houston 2000 X-Y recorder. A conventional two-compartment cell was used as the electrolytic cell. The salt bridge of the reference electrode was separated from the working electrode compartment by a Vycor glass. A platinum foil was used as the counter electrode. In aqueous media a saturated calomel electrode (s.c.e.) was used as the reference electrode. In non-aqueous media a Ag–$AgNO_3$ (0.1 mol dm^{-3} in MeCN) reference electrode was used, with the ferrocenium–ferrocene couple as the internal standard. The working electrodes used were either glassy carbon (Atomergic Chemetals V25) or platinum (Beckman Instruments, Inc.). Electrode surfaces were treated as previously described.[6]

Controlled-potential coulometry was performed using a PAR model 173 potentiostat and the quantity of electricity passed was measured by a PAR model 179 digital coulometer. The working electrode was a glassy carbon crucible (Atomergic Chemetals V25-12). During controlled-potential electrolysis the electrolyte was stirred with a synchronous stirring motor and purged with purified argon. U.v.–visible spectral changes were monitored by withdrawing aliquots of sample solution from the electrolytic cell during electrolysis.

Rotating-disc voltammetry was performed using a Pine Instrument model RDE4 bipotentiostat with a ASR-2 analytical rotator. Electrode treatment was as for cyclic voltammetry.

X-Ray Structure Determination.—Crystal data. The complex [Rh(bpb)$(py)_2$]ClO_4 crystallized as yellow hexagonal cylinders from acetonitrile by slow diffusion of diethyl ether, M = 676.87, space group $P\bar{1}$, a = 8.316(1), b = 9.620(2), c = 17.405(6) Å, α = 98.87(2), β = 99.57(2), γ = 90.55(2)°, U = 1 355.7(5) $Å^3$, D_c = 1.658 g cm^{-3}, Z = 2, μ(Mo-K_α) = 7.71 cm^{-1}, dimensions 0.36 × 0.24 × 0.10 mm.

Intensities (h, $\pm k$, $\pm l$; 5 258 unique data) were measured at 22 °C on a Nicolet R3m four-circle diffractometer (graphite-monochromatized Mo-K_α radiation, λ = 0.710 69 Å) using the ω—2θ variable-scan (2.02—8.37° min^{-1}) technique in the bisecting mode up to $2\theta_{max.}$ = 52°. Azimuthal scans of selected strong reflections over a range of 2θ values were used to define a pseudo-ellipsoid for the application of absorption corrections (μr = 0.08, transmission factors 0.722—0.937).[7–10]

Atomic co-ordinates for the Rh atom were deduced from a sharpened Patterson function, and the other non-hydrogen atoms were located from subsequent Fourier difference maps. All non-hydrogen atoms were refined anisotropically. The aromatic and pyridine H atoms were generated geometrically (C–H fixed at 0.96 Å) and allowed to ride on their respective parent carbon atoms; H atoms at calculated positions were included in structure-factor evaluation.

All computations were performed on a Data General Nova 3/12 minicomputer with the SHELXTL programs.[9] Analytical expressions of neutral-atom scattering factors incorporating the real and imaginary components of anomalous dispersion were employed.[10] Convergence for 4 788 observed data ($|F_o| > 3\sigma|F_o|$) and 379 variables was reached at R = 0.039, R' = 0.051, and S = 1.673 with weighting scheme $w = [\sigma^2(F_o) + 0.0005|F_o|^2]^{-1}$. The final Fourier difference map showed residual extrema in the range +0.78 to −0.91 $eÅ^{-3}$.

Atomic co-ordinates for non-hydrogen atoms are listed in Table 1, bond distances and angles in Table 2.

Additional material available from the Cambridge Crystallographic Data Centre comprises H-atom co-ordinates and thermal parameters.

Results and Discussion

Syntheses and Characterization.—In the preparation of Rh(bpb) complexes, refluxing H_2bpb and $RhCl_3$ in dimethylformamide (dmf) gave $[Rh(bpb)Cl_2]^-$ which was used as the starting material for subsequent syntheses. In the syntheses of $[Rh(bpb)(py)_2]^+$ and [Rh(bpb)(py)Cl] the reaction was accelerated by the presence of zinc powder; presumably, a rhodium(I) species generated *in situ* catalysed the substitution reaction. Reaction between $[Rh(bpb)Cl_2]^-$ and PPh_3 gave [Rh(bpb)(PPh_3)Cl] and $[Rh(bpb)(PPh_3)_2]^+$, the relative proportion of which depended on the reaction time and PPh_3 concentration. The complex [Rh(bpb)(PPh_3)Cl] has a low solubility in ethanol and easily precipitates from the reaction mixture, thus allowing easy separation of the two products. However, in the presence of a small amount of sodium hydroxide, the substitution reaction was driven to completion and $[Rh(bpb)(PPh_3)_2]^+$ became the sole product.

In this work the organorhodium complexes have been synthesized by reduction of Na[Rh(bpb)Cl_2] and Na[Rh(bpc)Cl_2]

Table 1. Atomic co-ordinates ($\times 10^5$ for Rh, $\times 10^4$ for other atoms) of $[Rh(bpb)(py)_2]ClO_4$

Atom	*x*	*y*	*z*	Atom	*x*	*y*	*z*
Rh	41 508(3)	19 458(3)	22 268(1)	C(15)	85(5)	3 598(5)	3 150(3)
O(1)	7 511(4)	859(4)	811(2)	C(16)	111(5)	3 199(5)	3 879(3)
O(2)	258(4)	4 307(3)	1 630(2)	C(17)	1 307(5)	2 350(4)	4 156(2)
N(1)	6 204(3)	882(3)	2 664(2)	C(18)	2 475(4)	1 932(4)	3 712(2)
N(2)	5 299(3)	1 815(3)	1 316(2)	N(5)	5 352(3)	3 828(3)	2 751(2)
N(3)	2 538(3)	2 981(3)	1 591(2)	C(19)	5 691(5)	4 109(4)	3 540(2)
N(4)	2 481(3)	2 325(3)	3 004(2)	C(20)	6 456(6)	5 331(4)	3 944(3)
C(1)	6 681(4)	512(4)	3 377(2)	C(21)	6 910(8)	6 312(5)	3 523(3)
C(2)	8 118(4)	−169(4)	3 555(2)	C(22)	6 569(7)	6 039(5)	2 708(3)
C(3)	9 057(5)	−519(4)	2 993(2)	C(23)	5 801(5)	4 803(4)	2 345(2)
C(4)	8 573(5)	−143(4)	2 255(2)	N(6)	2 950(3)	51(3)	1 751(2)
C(5)	7 166(4)	583(4)	2 110(2)	C(24)	2 965(4)	−972(4)	2 207(2)
C(6)	6 670(4)	1 091(4)	1 325(2)	C(25)	2 187(5)	−2 259(4)	1 942(2)
C(7)	4 469(4)	2 482(4)	706(2)	C(26)	1 319(5)	−2 523(4)	1 182(2)
C(8)	5 015(5)	2 578(4)	4(2)	C(27)	1 298(5)	−1 483(4)	714(2)
C(9)	4 128(5)	3 286(5)	−542(2)	C(28)	2 128(4)	−219(4)	1 012(2)
C(10)	2 704(5)	3 934(4)	−402(2)	Cl	7 312(2)	2 276(2)	5 630(1)
C(11)	2 126(5)	3 844(4)	291(2)	O(3)	6 375(9)	2 732(7)	5 044(3)
C(12)	3 005(4)	3 130(4)	855(2)	O(4)	6 612(15)	1 311(10)	5 896(7)
C(13)	1 295(4)	3 548(4)	1 910(2)	O(5)	7 549(13)	3 143(11)	6 308(4)
C(14)	1 278(4)	3 150(4)	2 719(2)	O(6)	8 659(11)	1 668(14)	5 410(4)

Table 2. Bond lengths (Å) and angles (°) of $[Rh(bpb)(py)_2]ClO_4$

Rh–N(1)	2.094(3)	Rh–N(2)	1.971(3)	C(9)–C(10)	1.383(6)	C(10)–C(11)	1.384(6)
Rh–N(3)	1.971(3)	Rh–N(4)	2.091(3)	C(11)–C(12)	1.396(5)	C(13)–C(14)	1.518(6)
Rh–N(5)	2.064(3)	Rh–N(6)	2.056(3)	C(14)–C(15)	1.374(6)	C(15)–C(16)	1.378(7)
O(1)–C(6)	1.219(5)	O(2)–C(13)	1.223(5)	C(16)–C(17)	1.366(6)	C(17)–C(18)	1.365(6)
N(1)–C(1)	1.341(5)	N(1)–C(5)	1.352(5)	N(5)–C(19)	1.339(4)	N(5)–C(23)	1.344(5)
N(2)–C(6)	1.341(5)	N(2)–C(7)	1.411(4)	C(19)–C(20)	1.365(5)	C(20)–C(21)	1.368(7)
N(3)–C(12)	1.427(5)	N(3)–C(13)	1.335(5)	C(21)–C(22)	1.382(7)	C(22)–C(23)	1.357(6)
N(4)–C(14)	1.359(4)	N(4)–C(18)	1.344(5)	N(6)–C(28)	1.338(4)	N(6)–C(24)	1.354(5)
C(1)–C(2)	1.381(5)	C(2)–C(3)	1.355(6)	C(24)–C(25)	1.369(5)	C(25)–C(26)	1.382(5)
C(3)–C(4)	1.385(6)	C(4)–C(5)	1.375(5)	C(26)–C(27)	1.382(6)	C(27)–C(28)	1.376(5)
C(5)–C(6)	1.516(5)	C(7)–C(8)	1.388(6)	Cl–O(3)	1.311(6)	Cl–O(4)	1.276(12)
C(7)–C(12)	1.417(5)	C(8)–C(9)	1.374(6)	Cl–O(5)	1.321(7)	Cl–O(6)	1.353(10)
N(1)–Rh–N(2)	80.8(1)	N(1)–Rh–N(3)	165.1(1)	C(8)–C(7)–C(12)	119.4(3)	N(2)–C(7)–C(12)	115.7(3)
N(2)–Rh–N(3)	84.4(1)	N(1)–Rh–N(4)	113.9(1)	C(8)–C(9)–C(10)	121.3(4)	C(7)–C(8)–C(9)	119.9(4)
N(2)–Rh–N(4)	165.3(1)	N(3)–Rh–N(4)	81.0(1)	C(10)–C(11)–C(12)	119.8(4)	C(9)–C(10)–C(11)	120.0(4)
N(1)–Rh–N(5)	89.0(1)	N(2)–Rh–N(5)	92.2(1)	C(7)–C(12)–C(11)	119.6(3)	N(3)–C(12)–C(7)	115.6(3)
N(3)–Rh–N(5)	89.7(1)	N(4)–Rh–N(5)	88.9(1)	O(2)–C(13)–C(14)	120.5(4)	N(3)–C(12)–C(11)	124.8(3)
C(7)–Rh–N(5)	91.6(1)	C(12)–Rh–N(5)	90.2(1)	N(4)–C(14)–C(13)	117.7(3)	O(2)–C(13)–N(3)	128.0(4)
N(1)–Rh–N(6)	90.1(1)	N(2)–Rh–N(6)	89.9(1)	C(13)–C(14)–C(15)	121.4(3)	N(3)–C(13)–C(14)	111.5(3)
N(3)–Rh–N(6)	91.8(1)	N(4)–Rh–N(6)	89.4(1)	C(15)–C(16)–C(17)	119.5(4)	N(4)–C(14)–C(15)	120.9(4)
C(7)–Rh–N(6)	90.8(1)	C(12)–Rh–N(6)	92.0(1)	N(4)–C(18)–C(17)	121.9(3)	C(14)–C(15)–C(16)	119.3(4)
N(5)–Rh–N(6)	177.6(1)	Rh–N(1)–C(1)	130.7(2)	Rh–N(5)–C(23)	123.6(2)	C(16)–C(17)–C(18)	119.4(4)
Rh–N(1)–C(5)	110.5(2)	C(1)–N(1)–C(5)	118.8(3)	N(5)–C(19)–C(20)	123.2(4)	Rh–N(5)–C(19)	118.6(2)
Rh–N(2)–C(6)	119.2(2)	Rh–N(2)–C(7)	112.4(2)	C(20)–C(21)–C(22)	119.1(4)	C(19)–N(5)–C(23)	117.7(3)
C(6)–N(2)–C(7)	128.3(3)	Rh–N(3)–C(12)	111.8(2)	N(5)–C(23)–C(22)	122.1(4)	C(19)–C(20)–C(21)	118.4(4)
Rh–N(3)–C(13)	118.9(2)	C(12)–N(3)–C(13)	128.9(3)	Rh–N(6)–C(24)	118.9(2)	C(21)–C(22)–C(23)	119.4(5)
Rh–N(4)–C(14)	110.5(2)	Rh–N(4)–C(18)	130.5(2)	N(6)–C(24)–C(25)	122.9(3)	Rh–N(6)–C(28)	123.1(2)
C(14)–N(4)–C(18)	118.9(3)	N(1)–C(1)–C(2)	121.7(3)	C(25)–C(26)–C(27)	118.5(3)	C(28)–N(6)–C(24)	117.9(3)
C(1)–C(2)–C(3)	119.8(4)	C(2)–C(3)–C(4)	118.8(4)	N(6)–C(28)–C(27)	122.0(3)	C(26)–C(25)–C(24)	118.8(4)
C(3)–C(4)–C(5)	119.6(4)	N(1)–C(5)–C(4)	121.2(3)	O(3)–Cl–O(5)	115.6(5)	C(26)–C(27)–C(28)	119.7(3)
N(1)–C(5)–C(6)	118.2(3)	C(4)–C(5)–C(6)	120.6(3)	O(3)–Cl–O(6)	112.4(5)	O(3)–Cl–O(4)	112.8(6)
O(1)–C(6)–N(2)	128.5(4)	O(1)–C(6)–C(5)	120.5(3)	O(5)–Cl–O(6)	115.8(6)	O(4)–Cl–O(5)	94.3(7)
N(2)–C(6)–C(5)	111.0(3)	N(2)–C(7)–C(8)	124.8(3)			O(4)–Cl–O(6)	103.9(8)

with $NaBH_4$, followed by nucleophilic displacement of halide from alkyl halide. The reduction of $[Rh(bpb)Cl_2]^-$ or [Rh(bpb)(py)Cl] took place readily at room temperature while a higher temperature of *ca.* 50 °C is required for $[Rh(bpc)Cl_2]^-$ reduction. In both cases, the resulting brown reduced products are insoluble, typical of rhodium(I) complexes of dianionic ligands. The rhodium(I) species are strong nucleophiles and react readily with alkyl halides to give the corresponding organorhodium complexes. Reaction of the rhodium(I) species with unsaturated hydrocarbons led to the net addition of Rh–H to the multiple bond. Styrene reacts with the rhodium(I) complex of the bpb ligand to give the 1-phenylethylrhodium complex (Scheme). Similarly, reaction between the rhodium(I) species and acrylonitrile gave the cyanoethylrhodium derivative,

Table 3. Proton n.m.r. spectral data of some organorhodium(III) complexes [M(L)R], (L = bpb, bpc, or bpe) in CD_3OD *

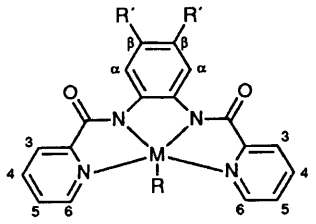

R' = H bpb
R' = Cl bpc

Complex		Proton signals of bpb system				
M	R	H_β	H_α	H^6	$H^{3,4,5}$	Proton signals of axial ligand
Rh	Me	6.99 (dd, 2 H, J_m = 3.50, J_o = 6.13)	8.62 (dd, 2 H, J_m = 3.50, J_o = 6.13)	8.93 [d, 2 H, $J(H^5H^6)$ = 5.25]	7.6—8.3 (m, 6 H)	0.92 [d, 3 H, J(RhH) = 2.63, CH_3]
Rh	Et	6.99 (dd, 2 H, J_m = 3.50, J_o = 6.13)	8.61 (dd, 2 H, J_m = 3.50, J_o = 6.13)	8.93 [d, 2 H, $J(H^5H^6)$ = 5.25]	7.6—8.3 (m, 6 H)	2.03 [dq, 2 H, J = 7.4, J(RhH) = 3.07, CH_2] 0.36 (t, 3 H, J = 7.4, CH_3)
Rh	Pr^i	7.00 (dd, 2 H, J_m = 3.50, J_o = 6.13)	8.62 (dd, 2 H, J_m = 3.50, J_o = 6.13)	8.98 [d, 2 H, $J(H^5H^6)$ = 5.25]	7.5—8.3 (m, 6 H)	2.65[doublehept.,1H,J = 6.56,J(RhH) = 3.06,CH] 0.52 (d, 6 H, J = 6.56, CH_3)
Rh	Ph(Me)CH–					3.77 [dq, 1 H, J = 7.4, J(RhH) = 3.5, CH] 0.76 [dd, 3 H, J = 7.4, J(RhH) = 1.3, CH_3]
		Proton signals of bpc system				
		H_α	H^6	$H^{3,4,5}$		
Rh	Me	8.74 (s, 2 H)	8.94 [d, 2 H, $J(H^5H^6)$ = 4.82]	7.6—8.3 (m, 6 H)		0.95 [d, 3 H, J(RhH) = 2.62, CH_3]
Rh	Et	8.73 (s, 2 H)	8.94 [d, 2 H, $J(H^5H^6)$ = 4.82]	7.6—8.3 (m, 6 H)		2.06 [dq, 2 H, J = 7.44, J(RhH) = 3.01, CH_2] 0.37 (t, 3 H, J = 7.44, CH_3)
[Rh(bpe)Me]·H_2O						0.71 [d, J(RhH) = 2.63, CH_3]
[Rh(bpe)Et]·H_2O						1.79 [dq, J = 7.4, J(RhH) = 2.5, CH_2] 0.28 (t, J = 7.4, CH_3)

* Chemical shifts δ are with reference to $SiMe_4$ in CD_3OD solution. Coupling constants, J, are in Hz.

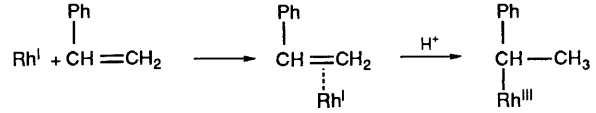

Scheme.

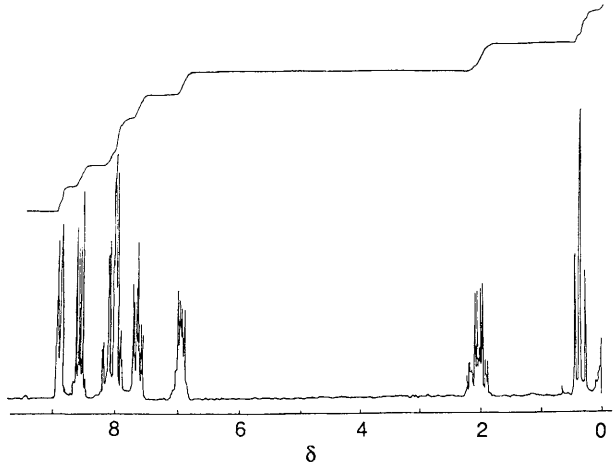

Figure 1. Proton n.m.r. spectrum of [Rh(bpb)Et]·H_2O in CD_3OD

which shows an intense i.r. absorption at 2 250 cm^{-1}, typical of ν(C≡N) for an organonitrile group.[11]

The organorhodium complexes of bpe were similarly prepared by $NaBH_4$ reduction followed by addition of alkyl halide. However, unlike the case of bpb and bpc, the reduction process had to be carried out at 0 °C to retard the demetallation reaction, indicating that the bpb and bpc ligands may have a higher co-ordination strength than bpe. However, pure products of bpe suitable for elemental analyses have not been obtained due to the hygroscopicity of the products.

Refluxing $Na_2[IrCl_6]$ and H_2bpb in dmf produced Na[Ir(bpb)Cl_2], which is soluble in methanol, acetone, and acetonitrile. Similarly, Na[Ir(bpc)Cl_2] could be isolated by refluxing $Na_2[IrCl_6]$ and H_2bpc in dmf. Due to the inertness of the dichloroiridium complexes toward substitution reactions, there is only limited reaction with pyridine and virtually no reaction with sodium cyanide. Attempts have been made to prepare organoiridium complexes. Addition of $NaBH_4$ to Na[Ir(bpb)Cl_2] or Na[Ir(bpc)Cl_2] in alkaline ethanol under a nitrogen atmosphere did not yield the hydride nor the iridium(I) species both at room temperature and at *ca.* 50 °C. Upon subsequent addition of alkyl halide no organoiridium complex could be isolated.

The newly prepared metal complexes are all air-stable solids and have satisfactory elemental analyses. Their i.r. spectra all

Table 4. Proton n.m.r. spectral data of some non-organo derivatives of rhodium and iridium

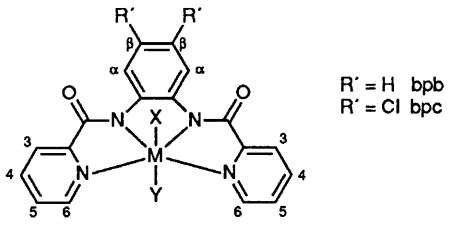

Complex			Proton signals of bpb system[a]			
M	X	Y	H_β	H_α	H^6	$H^{3,4,5}$
Rh	PPh_3	PPh_3[b]	6.7—8.0 (m) overlap with axial phenyl protons	8.39 (dd, 2 H, J_m = 3.50, J_o = 6.12)	8.91 [d, 2 H, $J(H^5H^6)$ = 4.81]	6.7—8.0
Rh	CN^-	CN^-[c]	7.04 (dd, 2 H, J_m = 3.50, J_o = 6.13)	8.68 (dd, 2 H, J_m = 3.50, J_o = 6.13)	9.08 [d, 2 H, $J(H^5H^6)$ = 5.25]	7.6—8.3 (m, 6 H)
Rh	Cl^-	Cl^-[c]	7.03 (dd, 2 H, J_m = 3.50, J_o = 6.13)	8.74 (dd, 2 H, J_m = 3.50, J_o = 6.13)	9.19 [d, 2 H, $J(H5H^6)$ = 5.68]	7.6—8.3 (m, 6 H)
Rh	py	py[b]	7.1—8.4 (m) overlap with axial pyridyl protons	8.85 (dd, 2 H, J_m = 3.50, J_o = 6.10)	9.37 [d, 2 H, $J(H^5H^6)$ = 5.49]	7.1—8.4
Ir	Cl^-	Cl^-[c]	6.9—7.1 (m)	8.6—8.8 (m)	9.10 [d, 2 H, $J(H^5H^6)$ = 5.25]	7.6—8.1 (m)

			Proton signals of bpc system[c]		
			H_α	H^6	$H^{3,4,5}$
Rh	CN^-	CN^-	8.79 (s, 2 H)	9.07 [d, 2 H, $J(H^5H^6)$ = 4.82]	7.7—8.4 (m, 6 H)
Rh	Cl^-	Cl^-	8.84 (s, 2 H)	9.19 [d, 2 H, $J(H^5H^6)$ = 4.82]	7.6—8.3 (m, 6 H)
Ir	Cl^-	Cl^-	8.85 (s, 2 H)	9.11 [d, 2 H, $J(H^5H^6)$ = 5.25]	7.6—8.1 (m, 6 H)

[a] Chemical shifts with reference to $SiMe_4$ in CD_3OD solution. Coupling constants, J, in Hz. [b] In CD_3CN. [c] In CD_3OD.

Table 5. Electronic absorption spectral data (sh = shoulder) for some rhodium and iridium complexes

Compound	$\lambda_{max.}$/nm ($\log_{10} \varepsilon_{max.}$)
[Rh(bpb)Me]·H_2O	436 (3.66), 333 (4.14), 259 (4.29), 196 (4.59)
[Rh(bpb)Et]·H_2O	414 (3.76), 309 (4.16), 259 (4.36), 196 (4.71)
[Rh(bpb)Pr^i]·H_2O	440 (3.62), 340 (4.13), 258 (4.32), 195 (4.74)
[Rh(bpb){CH(Me)(Ph)}]·H_2O	418(sh) (3.72), 308 (4.16), 250 (4.46), 197 (4.76)
[Rh(bpb)$(py)_2$]ClO_4	401 (3.79), 300(sh) (4.13), 258 (4.42), 196 (4.95)
[Rh(bpb)(py)Cl]	414 (3.70), 309 (4.05), 263 (4.22), 198 (4.81)
[Rh(bpb)$(PPh_3)_2$]ClO_4	402 (3.77), 308 (4.17), 260 (4.57), 204 (5.03)
[Rh(bpb)(PPh_3)Cl]	418 (3.77), 311 (4.09), 270 (4.56), 198 (5.01)
Na[Rh(bpb)$(CN)_2$]	418 (3.92), 310 (4.19), 255 (4.32), 195 (4.80)
Na[Rh(bpb)Cl_2]	426 (3.76), 323 (4.14), 265 (4.18), 199 (4.75)
Na[Ir(bpb)Cl_2]	460 (3.48), 333 (4.13), 259 (4.23), 197 (4.70)
[Rh(bpe)Me]·H_2O	378, 306, 248
[Rh(bpe)Et]·H_2O	383, 306, 250
[Rh(bpc)Me]·H_2O	430 (3.86), 331 (4.35), 261 (4.45), 195 (4.79)
[Rh(bpc)Et]·H_2O	412 (3.86), 300(sh) (4.29), 258 (4.42), 194 (4.78)
Na[Rh(bpc)$(CN)_2$]	411 (3.83), 302 (4.15), 257 (4.21), 194 (4.64)
Na[Rh(bpc)Cl_2]	419 (3.91), 322 (4.28), 273 (4.30), 202 (4.80)
Na[Ir(bpc)Cl_2]	450 (3.57), 333 (4.24), 260 (4.36), 194 (4.77)

show a ν(C=O) stretch at 1 610—1 635 cm^{-1}, which is at a lower frequency than that of the free ligand [ν(C=O): H_2bpb, 1 675m 1 665; H_2bpc, 1 710, 1 693 cm^{-1}]. This together with the absence of ν(N–H) stretches indicates that the two co-ordinated amide groups are depronated.

The ^1H n.m.r. spectral data for some alkylrhodium(III) complexes in CD_3OD are in table 3. The characteristic ^{103}Rh–^1H coupling constant confirms the presence of Rh–C bonding. Identification of the chemical shifts of methyl, ethyl-, and isopropyl- derivatives from the coupling pattern is straightforward. However, the phenyl-proton signals of the 1-phenylethyl derivative merge with the equatorial ligand signals. The chemical shifts and the J(Rh–H) values (≈3 Hz) are typical of rhodium complexes.[11,12] The chemical shift of the organo group of the alkylrhodium complexes of bpe is significantly different from that of bpb and bpc ligands, with the α- and β-carbon protons being shifted upfield, indicating the greater shielding effect of the Rh(bpe) moiety compared with Rh(bpb) and Rh(bpc). The splitting pattern of the pyridyl group of the bpe ligand is similar to that of bpb and bpc. The chemical shifts are also nearly identical. The protons of the ethylene bridge appear as a singlet at δ 3.85.

The ^1H n.m.r. spectra of some non-alkyl derivatives of rhodium and iridium were recorded either in CD_3OD or CD_3CN depending on the solubility of the complexes and the results are summarized in Table 4 (see also Figure 1). For the bpb ligand, chemical shifts and coupling constants of H_β were found to be virtually unaffected by the central metal ion and the axial ligand. Moreover, the nature of the solvent has no effect on the chemical shift of H_β. Although the chemical shifts and coupling constants of H_α and H^6 of the alkylrhodium complexes varied little with the alkyl groups studied, those of the non-alkyl derivatives varied significantly. In general, $\delta(H^6)$ changes in the same direction as $\delta(H_\alpha)$ but to a larger extent. The magnitude of the *cis* effect follows the order $H^6 > H_\alpha > H_\beta$ and may be ascribed to an inductive effect, which decreases with separation from the central metal ion.

In the presence of a large *cis* effect the influence of the central metal ions on the chemical shift can only be studied for complexes of identical axial ligands. Analyses of the n.m.r. data

Table 6. Summary of cyclic voltammetric data for the oxidation of 0.990 mmol dm^{-3} of $[Rh(bpb)Me]\cdot H_2O$ to $[Rh(bpb)Me]^+$ in acetonitrile with 0.1 mol dm^{-3} tetra-n-butylammonium fluoroborate as supporting electrolyte (working electrode: glassy carbon disc, area = 0.22 cm^2)

Scan rate, v/mV s^{-1}	Current ratio i_{p_c}/i_{p_a}	Current function, $i_{p_a}v^{-\frac{1}{2}}$/mA $s^{\frac{1}{2}}$ $V^{-\frac{1}{2}}$
200	0.98	0.227
100	0.96	0.227
50	0.94	0.227
20	0.90	0.233
10	0.84	0.240

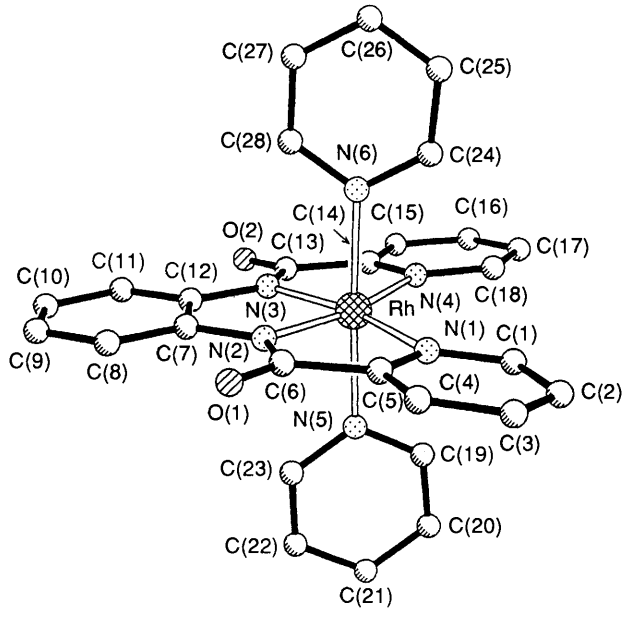

Figure 2. Perspective drawing showing the atom numbering and structure of the $[Rh(bpb)(py)_2]^+$ cation

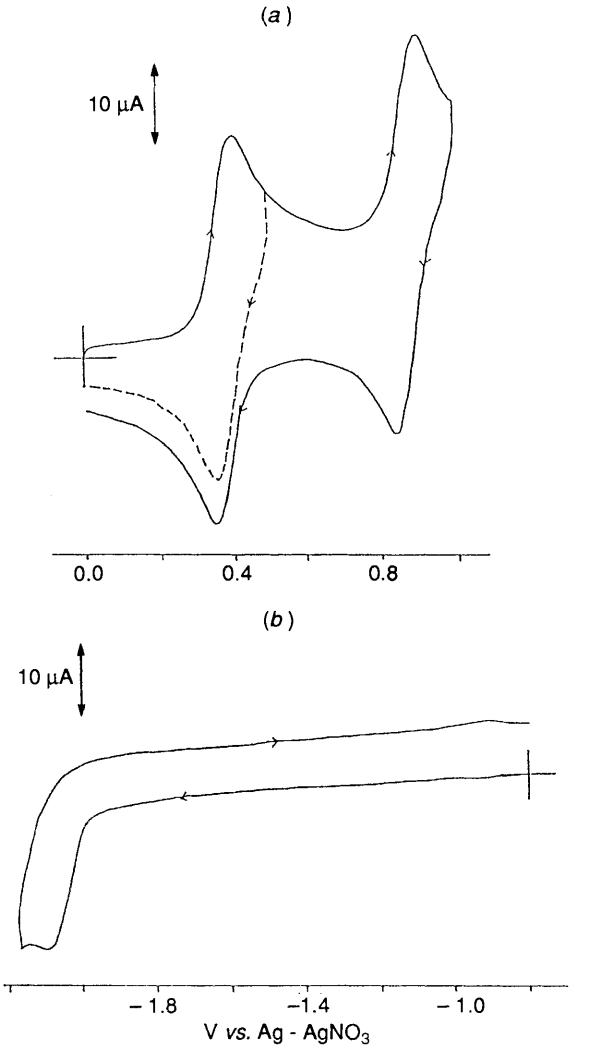

Figure 3. Cyclic voltammograms illustrating (*a*) the oxidation and (*b*) the reduction of $[Rh(bpb)Me]\cdot H_2O$ in acetonitrile. Working electrode, glassy carbon; supporting electrolyte, 0.1 mol dm^{-3} NBu_4BF_4; scan rate, 100 mV s^{-1}

for systems such as $[M(bpb)Cl_2]^-$ (M = Rh or Ir) showed that only $\delta(H^6)$ is affected to a significant extent, the trend being Rh > Ir. Similar findings were also made in the bpc system. The decrease of chemical shift down the group is just the opposite of that for the complexes [M(bpe)] (M = Ni, Pd, or Pt), with $\delta(H^6)$ increasing in the order Ni < Pd < Pt.[13] Due to the inductive effect of the chloro substituent, $\delta(H_a)$ shifts downfield for the bpc complexes of non-organo derivatives as in the case of organo derivatives.

The electronic absorption spectra of the rhodium and iridium complexes of bpb and bpc ligands all show intense bands (Table 5). The high absorption coefficients suggest either charge-transfer or intraligand transitions. The *d–d* transitions are not observed, probably being masked by the intense absorption bands.

X-Ray Structural Determination of $[Rh(bpb)(py)_2]ClO_4$.—The perspective drawing showing the atomic numbering and the structure of $[Rh(bpb)(py)_2]^+$ is shown in Figure 2. The octahedral structure of the complex has C_1 molecular symmetry. The Rh atom sits right in the mean plane of the four N atoms of the planar bpb ligand. The two axial pyridine ligands are perpendicular to the bpb ligand. However, the planes of the two pyridine rings do not bisect the benzene bridge symmetrically and also form a dihedral angle of 18.99° with each other resulting in the C_1 molecular symmetry. The Rh–N(py) bond distances are in the usual range.[14] However, the Rh–N(pyridyl of bpb) distances are about 0.03 Å longer than the Rh–N(py) bond distances. As in other bpb complexes, the Rh–N(amide) bond is much shorter than the Rh–N(pyridyl of bpb) bond.[15]

The N–C(amide) and N–C(bridge) bond distances of $[Rh(bpb)(py)_2]^+$ are similar to those in $[Cu(bpb)(H_2O)]$[15] but deviate from that of $[Cu(bpe)(H_2O)]$.[16] For the bpe ligand, delocalization of π electrons will mainly occur within the amide group and pyridine ring, which shortens the N–C(amide) bond and lengthens the C=O bond. On the other hand, with the introduction of a benzene bridge, the delocalization of π electrons across the entire bpb ligand will lengthen the N–C(amide) bond and shorten the N–C(bridge) bond. Moreover, the shorter N–C(bridge) bond in bpb complexes may also be accounted for by the sp^2 hybridization of the carbon atom relative to the sp^3 hybridization in the bpe complex. Thus, the different electrochemical oxidative behaviours of Rh(bpb) and Rh(bpe) complexes may be attributed to the ability of bpb complexes to delocalize charge throughout the π system, which stabilizes the ligand-centred radical cation.

Table 7. Cyclic voltammetric data for some rhodium complexes of bpb and bpc ligands in acetonitrile (0.1 mol dm^{-3} NBu_4BF_4; working electrode, glassy carbon; scan rate, 100 mV s^{-1}

	First oxidation		Second oxidation		First reduction	
Compound	$E^{0\,a}$	i_{p_c}/i_{p_a}	E^0 (E_{p_a})	i_{p_a2}/i_{p_a1} [b]	$E^0(E_{p_c})$	i_{p_c}/i_{p_aox} [c] (n) [d]
[Rh(bpb)Me]·H_2O	+0.31	0.99	+0.81	0.94	(−2.16)	0.87
[Rh(bpb)Et]·H_2O	+0.31	1.00	+0.82	0.94	(−2.20)	0.89
[Rh(bpb)Pr^i]·H_2O	+0.29	1.00	+0.83	0.96	(−2.20)	0.92
[Rh(bpb){CH(Me)(Ph)}]·H_2O	+0.30	0.95	+0.76	0.93	(−2.19)	0.95
Na[Rh(bpb)Cl_2]	+0.35	1.03	+0.91	0.85	(−1.98)	1.40
[Rh(bpb)$(py)_2$]ClO_4	+0.77	0.90	(+1.21)	2.10	(−1.70)	1.84 (1.80)
[Rh(bpb)(py)Cl]	+0.56	1.02	(+1.19)	1.75	(−1.87)	1.51
[Rh(bpb)(PPh_3)Cl]	+0.55	0.98	(+1.12)	2.05	(−1.62)	1.68
[Rh(bpb)$(PPh_3)_2$]ClO_4 [e]	+0.70	0.68	(+1.25)	1.81	(−1.30)	0.70 (0.96)
Na[Rh(bpb)$(CN)_2$]	+0.45	1.00	(+1.02)	1.10	(−2.31)	1.52
Na[Ir(bpb)Cl_2]	+0.21	0.98	+0.81	0.93	(−2.16)	1.86
[Rh(bpc)Me]·H_2O	+0.48	0.93	+0.94	0.91	−2.15	0.83
[Rh(bpc)Et]·H_2O	+0.46	1.03	+0.93	0.84	−2.16	0.83
Na[Rh(bpc)Cl_2]	+0.50	0.99	+0.99	0.85	−1.61	1.37
Na[Rh(bpc)$(CN)_2$]	+0.61	1.00	+1.07	0.87	−2.33	1.77
Na[Ir(bpc)Cl_2]	+0.31	0.99	+0.90	0.95	−2.12	1.83

[a] E^0 in V *vs.* ferrocenium–ferrocene is reported for reversible couples; E_{p_a} and E_{p_c} are reported for irreversible couples. [b] i_{p_a1} and i_{p_a2} are the peak currents of the first and second oxidation peaks respectively. [c] i_{p_c} and i_{p_aox} are the peak currents of the reduction and the first oxidation couple respectively. [d] n the number of electrons counted by controlled-potential coulometry. [e] Second reduction: $E_{p_c} = -1.50$ V, $i_{p_c}/i_{p_aox} = 0.62$ ($n = 1.94$).

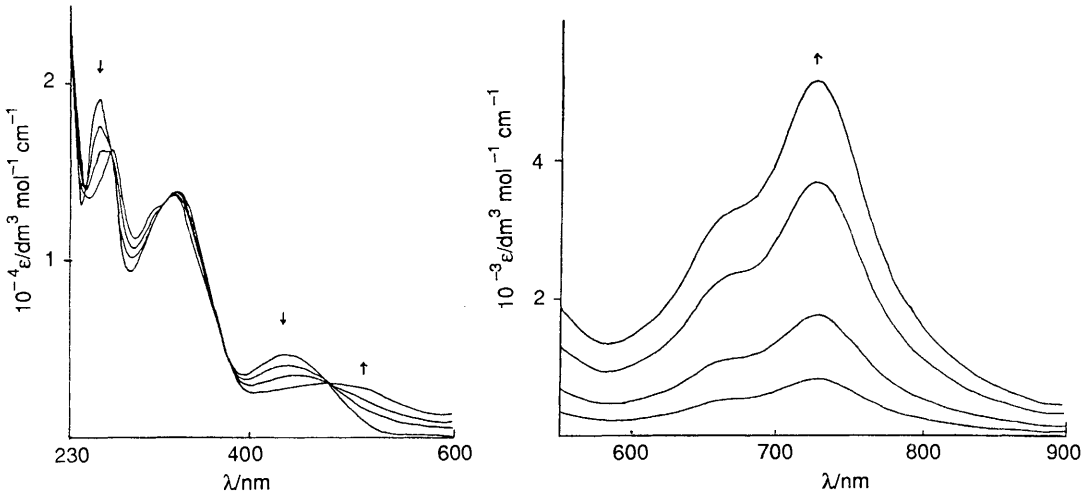

Figure 4. Electronic absorption spectra of [Rh(bpb)Me]·H_2O in 0.1 ml dm^{-3} NBu_4BF_3–MeCN during controlled-potential electrolysis at + 0.55 V *vs.* Ag–$AgNO_3$ (0.1 mol dm^{-3} in MeCN)

The C=O bond distances of $[Rh(bpb)(py)_2]^+$ are slightly shorter than those found in [Cu(bpb)(H_2O)],[15] [Cu(bpe)-(H_2O)]·H_2O,[16] and [Ni(bpe)]·H_2O.[17] This can be ascribed to the presence of hydrogen bonding between the water molecule and carbonyl group in the complexes of Cu and Ni, which weakens the C=O bond.

Electrochemistry.—The cyclic voltammogram of [Rh(bpb)-Me]·H_2O in acetonitrile exhibits two reversible oxidation couples at +0.31 and +0.81 V *vs.* ferrocenium–ferrocene, and an irreversible reduction couple at E_{p_c} of −2.16 V (Figure 3). Controlled-potential coulometry at +0.50 V *vs.* Ag–$AgNO_3$ (0.1 mol dm^{-3} in MeCN) showed that $n = 1.02$, establishing a one-electron oxidative process. The one-electron oxidized product has been characterized by u.v.–visible spectroscopy. Magnetic susceptibility measurement (Evans method) revealed $\mu_{eff.}$ of 1.83, characteristic of the spin-only value of one unpaired electron. During oxidation, the peaks at 259 and 430 nm decreased in intensity while intense absorptions appeared at 664 and 725 nm. Isosbestic points were observed at 268, 320, and 470 nm, showing that the oxidation was clean (Figure 4). The one-electron oxidation is reversible and occurs without secondary chemical reactions as the original electronic absorption spectrum can be regenerated upon electrochemical reduction of the oxidized product. The E_f^0 value is similar to the one-electron oxidation potential of the methylrhodium complex of *NN'*-ethylenebis(salicylideneiminate) (salen).[18]

Results of the scan rate dependence of the first oxidation couple are in Table 6. Between scan rates of 200 and 10 mV s^{-1} the peak-to-peak separation ΔE_p (60—70 mV) and the current function $i_{p_a}/v^{\frac{1}{2}}$ are relatively independent of the scan rate, v, typical of diffusion-controlled experiments with rapid simple one-electron transfer at the electrode without a preceding chemical reaction step. This is further supported by the observation of a linear Levich plot in rotating-disc voltammetric studies with a calculated diffusion coefficient of 17.0×10^{-3} cm^2

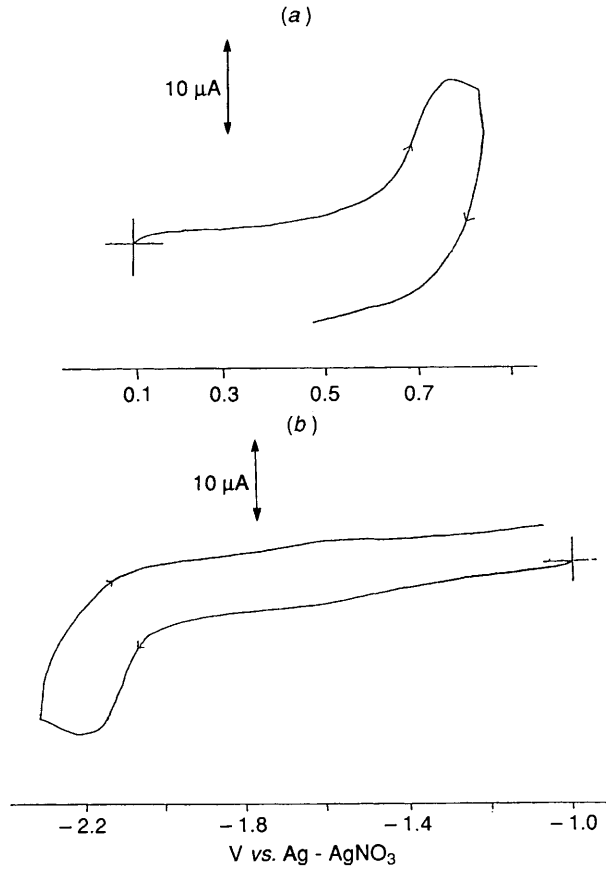

Figure 5. Cyclic voltammogram of $[Rh(bpe)Me]\cdot H_2O$ illustrating (*a*) the oxidation and (*b*) the reduction couples in acetonitrile, conditions as in Figure 3

s^{-1}. However, the current ratio i_{p_c}/i_{p_a} of the first oxidation couple is found to decrease from 0.98 at a scan rate of 200 mV s^{-1} to 0.84 at 10 mV s^{-1}, indicating a slow chemical reaction occurs after the electron transfer. A calculated n value of 1.18 has also been obtained from the combined results of scan-rate dependence and rotating-disc voltammetry, which agrees well with that obtained by controlled-potential coulometry. For the second oxidation couple a linear Levich plot is also obtained. A slope ratio of 0.99:1 between the Levich plots for the two oxidation couples established the one-electron transfer nature of the second oxidation couple. Determination of the value of n for this couple by controlled-potential coulometry was unsuccessful since the current did not drop to zero even after four electrons per mol had been passed. This is probably a result of the high instability and/or oxidizing power of the two-electron oxidized product.

Similarly, the cyclic voltammograms of other Rh(bpb) and Rh(bpc) complexes all show a reversible one-electron oxidation couple (Table 7). At a scan rate of 100 mV s^{-1} the current ratios, i_{p_c}/i_{p_a} of most complexes approach unity, indicating the stability of the one-electron oxidized product. The first oxidation couple of Rh(bpc) complexes is more anodic by 0.15 V than that of the corresponding Rh(bpb) complexes, demonstrating the electron-withdrawing effect of chlorosubstitution. However, with the exception of $[Rh(bpc)Cl_2]^-$, the reduction couples are virtually not affected by chlorosubstitution at the benzene bridge. A diffusion coefficient of 15.9×10^{-3} cm^2 s^{-1} has been obtained from the slope of the Levich plot for the first oxidation couple of $[Rh(bpc)Me]\cdot H_2O$, which is similar to that of $[Rh(bpb)Me]\cdot H_2O$. Except for the organorhodium complexes, the increase in the E_f^0 values parallels the increase in charge on the complex. For complexes bearing the same charge, the difference in E_f^0 is small. This indicates the dominance of the potential-energy terms over the effect of the donor strength of the axial ligands. The high strength of the alkyl ligand is reflected in the exceptionally low E_f^0 value.

Table 8. U.v.–visible spectral data (sh = shoulder) for one-electron-oxidized species of rhodium and iridium with bpb and bpc from cerium(IV) oxidation in MeCN solution

Compound	$\lambda_{max.}$/nm (10^{-3} $\varepsilon_{max.}$/dm^3 mol^{-1} cm^{-1})
$Na[Rh(bpb)(CN)_2]$	555(sh) (1.3), 614 (1.4)
$Na[Rh(bpb)Cl_2]$	750 (1.2), 82 (1.2)
$[Rh(bpb)(PPh_3)Cl]$	630 (1.4)
[Rh(bpb)(py)Cl]	710(sh) (0.9), 790 (1.8)
$[Rh(bpb)(py)_2]ClO_4$	530(sh), 570
$[Rh(bpb)Me]\cdot H_2O$	664 (3.2), 725 (5.2)
$[Rh(bpb)Et]\cdot H_2O$	680(sh) (1.7), 744 (2.6)
$[Rh(bpb)Pr^i]\cdot H_2O$	690(sh) (1.1), 758 (1.6)
$[Rh(bpb)\{CH(Me)(Ph)\}]\cdot H_2O$	660(sh) (1.0), 726 (1.5)
$Na[Rh(bpc)(CN)_2]$	596 (3.0), 648 (4.7)
$Na[Rh(bpb)Cl_2]$	780 (3.2), 860 (3.8)
$[Rh(bpc)Me]\cdot H_2O$	690 (3.7), 755 (7.1)
$[Rh(bpc)Et]\cdot H_2O$	700(sh) (2.1), 766 (3.8)
$Na[Ir(bpb)Cl_2]$	660 (1.5), 782 (2.2)
$Na[Ir(bpc)Cl_2]$	650 (1.5), 796 (2.9)

As in the case of organorhodium complexes of bpb and bpc ligands, the cyclic voltammograms of $[Rh(bpe)Me]\cdot H_2O$ and $[Rh(bpe)Et]\cdot H_2O$ exhibit irreversible reduction couples (Figure 5), with reduction potentials resembling that of the bpb and bpc complexes. This is consistent with the similar donor strengths of the three ligands and that the reduction is metal-centred, $Rh^{III} + e^- \longrightarrow Rh^{II}$. However, unlike the bpb and bpc complexes, the oxidation couple of $[Rh(bpe)R]\cdot H_2O$ has been shown to be irreversible and appears at a more anodic potential of around 0.63 V *vs.* ferrocenium–ferrocene. This suggests that the first oxidation couples of bpb and bpc complexes are largely ligand-centred since a similar potential and reversibility would be expected for all three complexes if the first oxidation couple is metal-centred. This is further supported by the relative insensitivity of the first oxidation couple of $[Rh(bpb)R]\cdot H_2O$ to the nature of the alkyl group and the relatively high stability of its one-electron oxidized product over that of Rh^{IV}(salen)R complexes.[18] Although H_2bpb only gives an irreversible oxidation peak at a much more anodic potential of 0.97 V *vs.* ferrocenium–ferrocene, co-ordination to metal and deprotonation of the amide groups in $[Zn(bpb)]\cdot H_2O$ can cause the bpb ligand to be oxidized at a less anodic potential of 0.40 V. Thus, the first oxidation couple of rhodium complexes of bpb and bpc ligands is postulated to involve largely ligand character with little metal contribution. In the bpe complexes ligand-centred oxidation is not possible. Thus, the irreversible nature of the oxidation couple in $[Rh(bpe)R]\cdot H_2O$ is likely to be metal-centred where the highly oxidizing rhodium(IV) species causes dissociation of the alkyl ligand or oxidation of the equatorial ligand.

Similar to the rhodium complexes $[Ir(bpb)Cl_2]^-$ and $[Ir(bpc)Cl_2]^-$ complexes show two reversible one-electron oxidation couples. The first oxidation couples are less anodic than those of the rhodium analogues by 0.14 and 0.19V, respectively. Thus, the metal centre may have a greater contribution to the redox orbital, in accordance with the ease of oxidation of the metal down a group in the periodic table.

Controlled-potential electrolysis of $[Ir(bpb)Cl_2]^-$ at +0.40 V *vs.* Ag–$AgNO_3$ (0.1 mol dm^{-3} in MeCN) showed $n = 0.94$, indicating that the couple is a one-electron oxidative process. The reduction reaction is irreversible. It involves a two-electron

transfer, possibly Ir^{III} to Ir^{I}, as suggested by the ratio of peak currents of the reduction and the first oxidation couple. The inertness of iridium complexes toward reduction is reflected in the reduction potentials which are more cathodic than those of the corresponding rhodium complexes. With chloro-substitution of the benzamide bridge in bpc, both the oxidation and reduction couples are found to shift anodically in the $[Ir(bpc)Cl_2]^-$ complex. However, the effect is smaller than that with the rhodium counterpart.

Redox Chemistry with Cerium(IV).—Cerium(IV) titration provides a quick method to generate the one-electron oxidized species. The products are found to be identical to that obtained from controlled-potential electrolyses. The stability of the one-electron oxidized species is in accordance with the current ratio, i_{p_c}/i_{p_a}, of the first oxidation couple. Thus, $[Rh(bpb)(py)_2]^+$ which has a current ratio of 0.90 at a scan rate of 100 mV s^{-1} shows intense absorption in the low-energy region during cerium(IV) titration, assignable to the cation radical of the benzamide bridge, which would be expected to resemble that of $tmpd^+$ ($\lambda_{max.} \approx 565$ nm, tmpd = *N*,*N*,*N*′,*N*′-tetramethyl-*p*-phenylenediamine).[19] However, the product was found to be unstable and the intensity of the absorption decreased gradually with time. The position of absorption peaks is found to be dependent upon the nature of the axial ligand where the absorption wavelength decreases in the order: $2Cl^- > (py)Cl > (Pr^i)H_2O > (Et)H_2O \approx [CH(Me)(Ph)]H_2O > (Me)H_2O \gg (PPh_3)Cl > 2CN^-$. Similar observations have been obtained for the Rh(bpc) complexes. Similarly, $[Ir(bpb)Cl_2]^-$ and $[Ir(bpc)Cl_2]^-$ complexes can be oxidized by cerium(IV) to species having sufficient stability to be monitored by visible spectroscopy. Two absorption peaks in the low-energy region are observed.

The dependence of absorption energies upon the nature of substituents on the equatorial ligand, axial ligands, and central metals is summarized in Table 8. The axial ligand may exert its effect through the central metal electron density which in turn affects the energy levels and electron density on the equatorial ligand. This is in accordance with the postulation based upon electrochemical studies that the redox orbital of the first oxidation couple is mainly ligand-centred but has a certain degree of metal character.

Acknowledgements

We acknowledge support from the University of Hong Kong and the University and Polytechnic Grants Committee.

References

1 E. C. Constable, *Coord. Chem. Rev.*, 1986, **73**, 113.
2 J. Halpern, M. S. Chan, J. Hanson, T. S. Roche, and J. A. Topich, *J. Am. Chem. Soc.*, 1975, **97**, 1606; J. Halpern, J. Topich, and K. I. Zamaraev, *Inorg. Chim. Acta*, 1976, **20**, L21; R. H. Magnuson, J. Halpern, I. Y. Levitin, and M. E. Volpin, *J. Chem. Soc., Chem. Commun.*, 1978, 44; J. Halpern, M. S. Chan, T. S. Roche, and G. M. Tou, *Acta Chem. Scand.*, 1979, 141; J. A. Topich and J. Halpern, *Inorg. Chem.*, 1979, **18**, 1339.
3 D. J. Barnes, R. L. Chapman, R. S. Vagg, and E. C. Watton, *J. Chem. Eng. Data*, 1978, **23**, 349.
4 R. L. Chapman and R. S. Vagg, *Inorg. Chim. Acta*, 1979, **33**, 227.
5 W. T. Wong, M.Phil. Thesis, University of Hong Kong, 1988.
6 C. M. Che, K. Y. Wong, and F. C. Anson, *J. Electroanal. Chem.*, 1987, **226**, 211.
7 G. Kopfmann and R. Huber, *Acta Crystallogr., Sect. A*, 1968, **24**, 348; A. C. T. North, D. C. Phillips, and F. S. Matthews, *ibid.*, p. 351.
8 J. S. Rollett, 'Crystallographic Computing,' ed. F. R. Ahmed, Munksgaard, Copenhagen, 1970, p. 167.
9 G. M. Sheldrick, 'Computational Crystallography,' ed. D. Sayre, Oxford University Press, New York, 1982, p. 506.
10 'International Tables for *X*-Ray Crystallography,' Kynoch Press, Birmingham, 1974.
11 J. H. Weber and G. N. Schrauzer, *J. Am. Chem. Soc.*, 1970, **92**, 726.
12 H. Ogoshi, J. I. Setsune, T. Omura, and Z. I. Yoshida, *J. Am. Chem. Soc.*, 1975, **97**, 6461; C. A. Rogers and B. O. West, *J. Organomet. Chem.*, 1974, **70**, 445; R. J. Cozens, K. S. Murray, and B. O. West, *ibid.*, 1972, **38**, 391; K. Thomas, J. A. Osborn, A. R. Powell, and G. Wilkinson, *J. Chem. Soc. A*, 1968, 1801.
13 D. J. Barnes, R. L. Chapman, F. S. Stephens, and R. S. Vagg, *Inorg. Chim. Acta*, 1981, **51**, 155.
14 P. Colamarino and P. Orioli, *J. Chem. Soc., Dalton Trans.*, 1976, 845; B. M. Gatehouse, R. E. Reicher, and B. O. West, *Acta Crystallogr., Sect. B*, 1976, **32**, 30; J. Roziers, M. S. Lehmann, and J. Potier, *ibid.*, 1979, **35**, 1099.
15 R. L. Chapman, F. S. Stephens, and R. S. Vagg, *Inorg. Chim. Acta*, 1980, **43**, 29.
16 R. L. Chapman, F. S. Stephens, and R. S. Vagg, *Acta Crystallogr., Sect. B*, 1981, **37**, 75.
17 F. S. Stephens and R. S. Vagg, *Inorg. Chim. Acta*, 1982, **57**, 9.
18 I. Y. Levitin, A. L. Sigan, and M. E. Volpin, *J. Chem. Soc., Chem. Commun.*, 1975, 469.
19 G. T. Pott and J. Kammandeur, *J. Chem. Phys.*, 1969, **47**, 395; A. C. Albrecht and W. T. Simpson, *J. Am. Chem. Soc.*, 1955, **77**, 4454.

Received 8*th December* 1989; *Paper* 9/05253D